SOME EFFECTS WHICH ARISE IN CONNECTION WITH THE EXPLOSIVE SQUEEZING OF A VISCOUS CYLINDRICAL SHELL

N. I. Tatyushkin and Yu. A. Trishin

UDC 532.52+532.503.2

The process of the collapse of a cylindrical metal shell to the axis of symmetry under the action of explosion products has been discussed in [1-3]. The model of an ideal incompressible fluid has been taken as the basis for calculations of a collapsing shell. Comparison of the results of a numerical solution of the problem of the convergence of ideal incompressible fluid to the axis of the shell with experimental data obtained in connection with photography by an x-ray pulse apparatus of the collapse process of metal tubes surrounded by a layer of explosives shows that the calculated curves of the time dependence of the shell radius are in good agreement with the experimental times up to a certain point. An appreciable divergence begins at the end of the process of shell collapse. The divergence with experiment was overcome by using the model of a viscous incompressible fluid for the shell material. In addition, this model explained a number of physical effects which were first obtained experimentally: the halting of the shell upon reaching an inner surface of some critical radius not equal to zero, the "explosive" vaporization of the shell due to the rapid conversion of all the kinetic energy of the shell into heat due to the action of viscous forces, and the dynamical stability loss of the shell. The elastoplastic model is not able to explain these phenomena which accompany the collapse process of a cylindrical shell.

Thus, the viscosity of actual shells is evidently the principal factor limiting accumulation (in the sense of a collision of the inner surface on the symmetry axis) in shells with cylindrical symmetry. But at the same time it is possible to speak of another kind of accumulation in the model discussed below – the accumulation of thermal energy in the layers adjacent to the inner surface, which, in turn, is limited by phase transitions of the shell material. A procedure for determining the viscosity coefficients for metal and other condensed materials is proposed on the basis of an analysis of the inertial convergence of a cylindrical shell.

A suggestion is made in this paper on the nature of the high-velocity cumulative jet from cylindrical cumulative casings and about the converging cylindrical detonation front.

§1. Let there be a cylindrical shell of a viscous incompressible fluid surrounded by a layer of compressed gas. The initial parameters of the gas are as follows: pressure p_0, density ρ_0, sound velocity in the gas a_0, and layer thickness Δ_0; those of the shell are as follows: density of the material ρ_1, dynamic viscosity coefficient μ, inner radius R_0, and outer radius R_{10}. There is a vacuum inside and outside the layer of compressed gas. The shell will start to collapse under the influence of the expanding gas.

Assuming that the gas surrounding the cylindrical shell is the product of the instantaneous detonation of explosives with $\gamma = 3$, it is possible to write [1-4]:

$$p_0 = \frac{1}{8}\rho_0 D^2 = \frac{1}{3}\rho_0 a_0^2,\ \rho_0 = \rho_{\text{expl}}, \tag{1.1}$$

where D is the detonation velocity of the explosives and ρ_{expl} is the initial density of the explosives.

The condition of adiabaticity gives the following relationship for the thermodynamic parameters of the gas:

$$\rho = \rho_0 a/a_0,\ p = p_0(\rho/\rho_0)^3 = p_0(a/a_0)^3. \tag{1.2}$$

The equations of motion and continuity describing the one-dimensional motion of the gas with cylindrical symmetry are transformed, with Eqs. (1.2) taken into account, into equations containing the mass velocity u and the speed of sound a as the desired functions:

$$\partial u/\partial t + u\partial u/\partial r + a\partial a/\partial r = 0,\ \partial a/\partial t + u\partial a/\partial r + a\partial u/\partial r + au/r = 0. \tag{1.3}$$

Novosibirsk. Translated from Zhurnal Prikladnoi Mekhaniki i Tekhnicheskoi Fiziki, No. 3, pp. 99-112, May-June, 1978. Original article submitted May 13, 1977.

 0021-8944/78/1903-0362$07.50

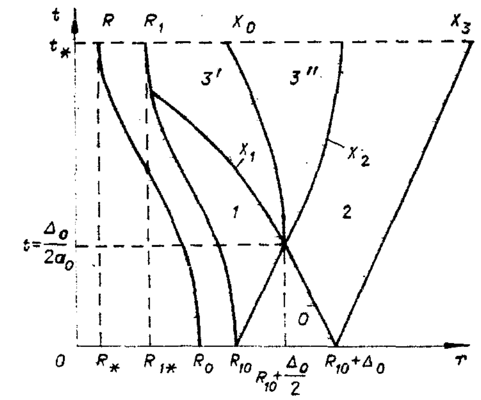

Fig. 1

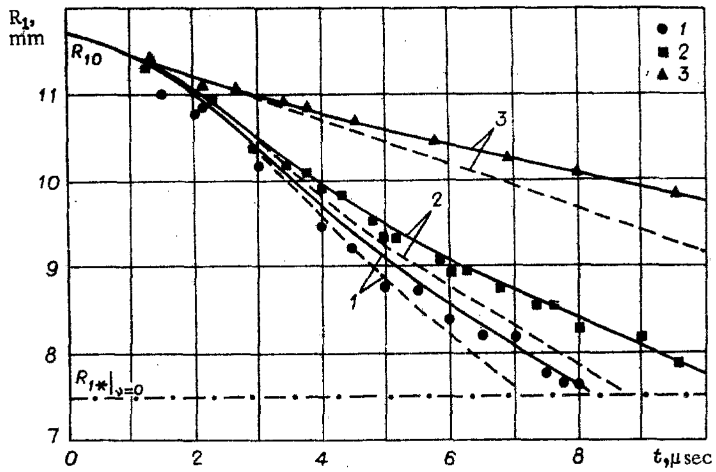

Fig. 2

Let us consider the r−t diagram of the collapse process of a cylindrical shell (Fig. 1). The trajectory of the inner and outer shell boundaries are denoted by R(t) and $R_1(t)$, respectively, $X_1(t)$ is the leading front of a rarefaction wave propagating to the left from the gas−vacuum boundary, and $X_2(t)$ is the leading front of a rarefaction wave propagating to the right and arising on the moving shell. The curves X_1 and X_2 have rectilinear sections up to their intersection point $[R_{10} + \Delta_0/2, \Delta_0/(2a_0)]$. The r axis and the rectilinear sections of the curves X_1 and X_2 restrict the region 0 of unperturbed gas, where u=0 and $a = a_0$. The gas−vacuum boundary $X_3(t)$ is a straight line, since not a single perturbation can overtake this boundary (for example, see [5]). The displacement velocity of this boundary is equal to the gas outflow velocity into the vacuum, which for $\gamma = 3$ is equal to the initial speed of sound in the gas. Thus, the region of moving gas in the r−t diagram is restricted by the shell line $R_1(t)$, the rectilinear sections of the leading fronts of the rarefaction waves X_1 and X_2, and by the line X_3 of gas dispersion into the vacuum. In its turn, this region can be divided into several parts [see Fig.1]: 1) the region of gas motion in the rarefaction wave which arises on the cylindrical shell; 2) the region of gas motion in the rarefaction wave which arises in connection with gas dispersion into the vacuum; 3) the region of interaction of the rarefaction waves generated. The region 3 is divided into two parts by the line $X_0(t)$: to the left of it (region 3') the gas velocity is directed toward the shell, and to the right (region 3"), the gas velocity is directed toward the gas−vacuum boundary. The mass velocity of the gas is equal to zero on the line X_0.

For the cylindrical shell itself relations expressing the law of mass conservation and the continuity equation for an incompressible fluid are satisfied:

$$R_1^2(t) - R^2(t) = R_{10}^2 - R_0^2 = C = \text{const}; \tag{1.4'}$$

$$R_1(t)\dot{R}_1(t) = R(t)\dot{R}(t) = rv. \tag{1.4"}$$

The initial conditions are obvious:

$$u(r, 0) = \dot{R}_1(0) = 0, \ a(r, 0) = a_0, \ R_1(0) = R_{10}, \ R(0) = R_0, \ X_3(0) = R_{10} + \Delta_0. \tag{1.5}$$

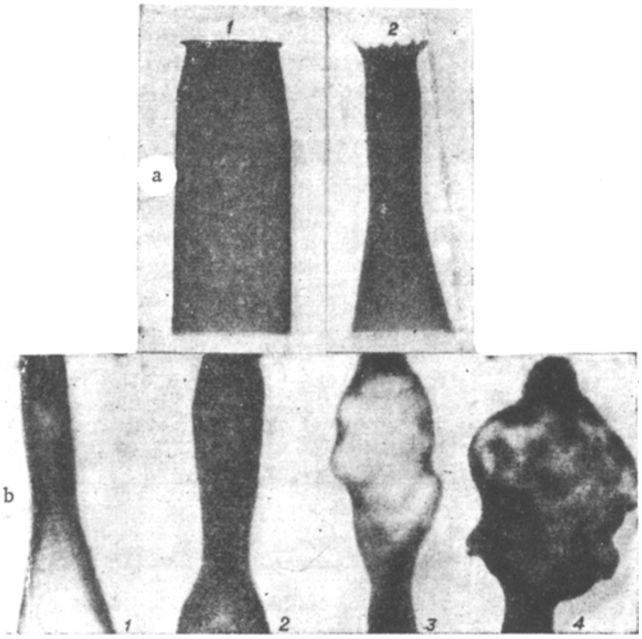

Fig. 3

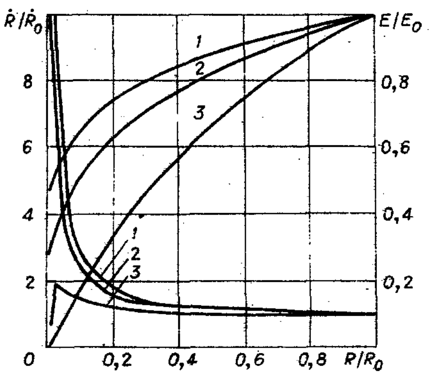

Fig. 4

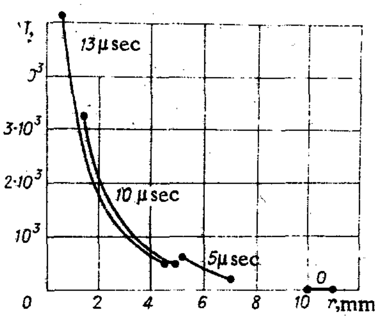

Fig. 5

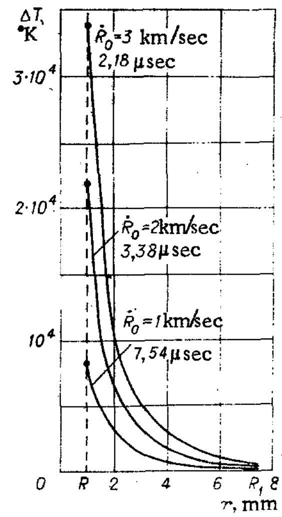

Fig. 6

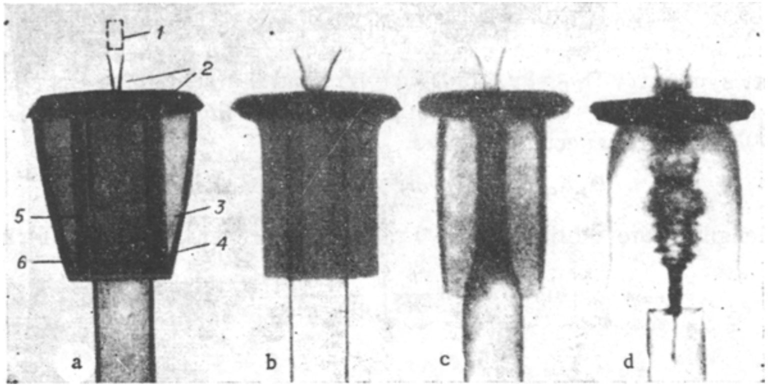

Fig. 7

Fig. 8

Let us write out the conditions at the boundary of the region of moving gas:

$$\begin{cases} \text{at} \quad X_3(t), \; u = a_0, \; a = 0; \\ \text{at} \quad X_1(t), \; X_2(t) \; \text{for} \quad 0 \leqslant t \leqslant \frac{\Delta_0}{2a_0} \quad u = 0, \; a = a_0; \\ \text{at} \quad R_1(t), \; u = \dot{R}_1, \; a = a_1. \end{cases} \tag{1.6}$$

In addition, a relation relating the acceleration of the shell to the parameters of the shell and the gas is satisfied on $R_1(t)$ which it is possible to derive from energy considerations.

Let us consider the conservation law of mechanical energy for some volume V of a continuous medium, which in the general case has the form

$$\frac{d}{dt} \int\limits_V \rho_1 \frac{v_i v_i}{2} \, dV + \int\limits_V D_{ij} \sigma_{ji} \, dV = \int\limits_S v_i t_i^{(n)} dS, \tag{1.7}$$

where ρ_1 is the density of the medium, v_i is the velocity vector of a material point, D_{ij} is the tensor of the deformation rates, σ_{ij} is the stress tensor, S is the surface bounding the volume V, and $t_i^{(n)} = \sigma_{ji} n_j$ is the stress vector at the small area dS with normal n.

Equation (1.7) establishes a relation between the rate of variation of the total mechanical energy of the medium and the strength of the surface forces. Let us apply Eq. (1.7) to the one-dimensional axisymmetric motion of a cylindrical shell converging to the axis under the influence of the gas pressure p on the outer surface of the shell (the gas pressure on the inner surface is p = 0). The shell is an incompressible Newtonian fluid for which:

$$\sigma_{ij} = -p\delta_{ij} + 2\mu D_{ij}.$$

In the case of cylindrical symmetry $D_{rr} = \partial v/\partial r$, $D_{\varphi\varphi} = v/r$, and the remaining $D_{ij} = 0$. In addition, $D_{ij}\sigma_{ji} = -pD_{ii} + 2\mu D_{ij}D_{ij} = 2\mu D_{ij}D_{ij}$, since $D_{ii} = 0$ by virtue of $\rho_1 = \text{const}$ and the continuity equation (1.4″). With the continuity equation (1.4″) taken into account we have

$$D_{ji}\sigma_{ji} = 2\mu[(\partial v/\partial r)^2 + (v/r)^2] = 4\mu R^2\dot{R}^2/r^4. \tag{1.8}$$

Then Eq. (1.7) for unit length of the shell with (1.4″) taken into account, takes the form

$$\frac{d}{dt}\left[\pi\rho_1(R\dot{R})^2 \ln\frac{R_1}{R}\right] + \frac{4\mu\pi C\dot{R}^2}{R_1^2} = -2\pi R\dot{R}p, \tag{1.9}$$

where $C = R_1^2 - R^2 = \text{const}$.

Differentiating the first term of Eq. (1.9) with respect to the time and using Eqs. (1.1) and (1.2), we finally obtain

$$\frac{d\dot{R}_1}{dt} = \frac{1}{R_1 \ln\frac{R_1}{R}}\left(\frac{C\dot{R}_1^2}{2R^2} - \frac{2\nu C\dot{R}_1}{R_1R^2} - \frac{\rho_0 a_1^3}{3\rho_1 a_0}\right) - \frac{\dot{R}_1^2}{R_1}, \tag{1.10}$$

where $\nu = \mu/\rho_1$ is the kinematic viscosity. Equation (1.10) is the boundary condition for the region of moving gas and is satisfied on the curve $R_1(t)$.

The solution of the equations of one-dimensional motion of a gas with cylindrical symmetry (1.3) with the initial (1.5) and boundary conditions (1.4′), (1.4″), (1.6), and (1.10) was constructed numerically by the modified method of characteristics described in [1-3]. The agreement of the calculated curves of the time dependence of the radius of the cylindrical shell with the experimental results was achieved by the choice of the value of the kinematic viscosity of the shell material. For copper the value of the kinematic viscosity turned out to be equal to $\nu = 0.7 \cdot 10^4$ cm²/sec, which is less than the kinematic viscosity cited in [6].

The calculated dependences of the radius of a collapsing copper cylindrical shell ($R_0 = 9$ mm, $R_{10} = 11.7$ mm, and $\rho_1 = 8.9$ g/cm³) under the action of a layer of explosives – an alloy of Trotyl with Hexogen, TH 50/50 ($\rho_{\text{expl}} = 1.65$ g/cm³, $D = 7.5$ km/sec, and $a_0 = 4.5$ km/sec) are presented in Fig. 2. The solid curves are plotted for a viscous shell with $\nu = 0.7 \cdot 10^4$ cm²/sec, and the dashed curves are for the model of an ideal incompressible fluid ($\nu = 0$). The curves 1-3 refer to different thicknesses of the explosives on the outer surface of the cylindrical shell ($\Delta_0 = 8.2$, 5.9, and 2.4 mm, respectively). The experimental results are plotted as points. The good overlapping of the experimental points by the calculated curves over the entire collapse process for the chosen kinematic viscosity coefficient and the appreciable discrepancy of the experimental points with the model of an ideal incompressible fluid at the end of the process argue in favor of the viscous incompressible fluid model.

§ 2. Let us consider the inertial collapse of a viscous cylindrical shell in which the gas pressure both on the outer and on the inner shell surfaces is equal to zero, and $R = R_0$, $R_1 = R_{10}$, and $\dot{R} = \dot{R}_0$ at $t = 0$. In this case from Eq. (1.9) we have

$$\frac{d}{dt}\left[\pi\rho_1(R\dot{R})^2 \ln\frac{R_1}{R}\right] = -\frac{4\pi\rho_1\nu C\dot{R}^2}{R_1^2}, \tag{2.1}$$

where $E = \pi\rho_1(R\dot{R})^2\ln(R_1/R)$ is the kinetic energy per unit length of the cylindrical shell.

Integrating (2.1) on the condition that $E = E_0$ at $R = R_0$, we obtain

$$\sqrt{E} = \sqrt{E_0} - 4\nu\sqrt{\pi\rho_1}\left(\sqrt{\ln\frac{R_1}{R}} - \sqrt{\ln\frac{R_{10}}{R_0}}\right). \tag{2.2}$$

Equation (2.2) indicates that $R = R_* \neq 0$ occurs when $E = 0$:

$$R_* = R_0\sqrt{\frac{(R_{10}/R_0)^2 - 1}{(R_{10}/R_0)^m - 1}}, \tag{2.3}$$

where $m = 2[1 + (\frac{R_0|\dot{R}_0|}{4\nu})]^2 = 2[1 + (\frac{\text{Re}}{4})]^2$. The stopping radius R_* of the shell at a certain distance from the symmetry axis is very small in the general case upon detonation of the explosives in contact with the shell due to a very strong dependence on the Reynolds number, which is defined in the form $\text{Re} = R_0|\dot{R}_0|/\nu$.

Actually, the stopping radius is found to be equal to $\sim 10^{-14}$ cm for a copper shell ($\nu = 0.7 \cdot 10^4$ cm^2/sec) with an inner radius of 50 mm and a thickness of 5 mm in the case of an initial collapse velocity of $\dot{R}_0 = 1$ km/sec. It is clear that it is impossible to detect such a value by any instrumental measurements. But the stopping radius R_* may prove to be appreciable for cylindrical shells for which $Re \to 0$. If we now take a copper shell having the same initial collapse velocity of 1 km/sec but a thickness of 0.5 mm and $R_0 = 5$ mm, then R_* turns out to be equal to 1.23 mm, and it is possible to record it by x-ray pulse photography.

It can be shown that if there are dissipative forces in the shell, then it is possible to obtain the stopping effect by the action, for example, of the resistive forces of the shell material. The case of the inertial convergence of an elastoplastic cylindrical shell toward the symmetry axis has been theoretically investigated in [7], and a minimum initial velocity $\dot{R}_{0*}$, has been found at which the shell collapses. The initial velocity $\dot{R}_{0*}$ turns out to be equal to 160 m/sec for a copper cylinder with $R_0 = 9$ mm and $R_{10} = 10$ mm whose yield point is $\sigma_S = 6.85 \cdot 10^8$ dyn/cm^2. In the case of the explosive squeezing of a copper shell at an initial velocity $\dot{R}_0$ of the order of 1 km/sec and higher, the elastoplastic model is not able to explain the stopping effect. The loss of energy in overcoming the plastic resistance of the material amounts to 2.5% in all of the initial kinetic energy of the shell in the case of $\dot{R}_0 = 1$ km/sec.

It is possible to treat the inertial collapse of an empty spherical cavity of radius R_0 in an unbounded incompressible viscous fluid in a similar formulation. In this case the continuity equation has the form $v = \dot{R}R^2/r^2$, and the components of the deformation rate tensor $D_{rr} = \partial v/\partial r$, $D_{\varphi\varphi} = D_{\theta\theta} = v/r$, and the remaining $D_{ij} = 0$ and $D_{ij}\sigma_{ji} = 2\mu D_{ij}D_{ij} = 12\mu\dot{R}^2R^4/r^6$. Therefore, one can write Eq. (1.7) in the form

$$dE/dt = -16\pi\mu\dot{R}^2R, \tag{2.4}$$

where $E = 2\pi\rho_1 R^3\dot{R}^2$ is the total kinetic energy. Eliminating the time and integrating (2.4) with the obvious initial conditions, we obtain

$$\sqrt{E} = \sqrt{E_0} - 8\nu\sqrt{2\pi\rho_1}(\sqrt{R_0} - \sqrt{R}). \tag{2.5}$$

In the case of inertial convergence to the center of the spherical cavity both collapse to zero radius and the stopping of the cavity at a certain distance from the center can occur in a viscous fluid. This depends on the initial conditions. Let us find the function R(t) from Eq. (2.5) in quadratures

$$t = \int_{R_0}^{R} \frac{R^{3/2}dR}{\sqrt{R_0}\left(R_0\dot{R}_0 + 8\nu\right) - 8\nu\sqrt{R}}. \tag{2.6}$$

We will consider three cases: 1) $R_0\dot{R}_0 + 8\nu = 0$, i.e., $Re = R_0|\dot{R}_0|/\nu = 8$; then we obtain $R_0^2 - R^2 = 16\nu t$ from (2.6), whence it follows that the cavity collapses to zero radius in the finite time $t_* = R_0^2/16\nu$, and $R \to 0$, $\dot{R} = -8\nu/R \to -\infty$, and $E = 128\pi\rho_1\nu^2R \to 0$ as $R \to 0$; 2) $R_0\dot{R}_0 + 8\nu > 0$, i.e., $Re < 8$; then we obtain from (2.6) that the denominator of the integrand is less than zero when $R \approx R_0$, and it is greater than zero when $R \to 0$; this fact indicates that for $R_* = (1 - Re/8)^2R_0$ the moving cavity stops, $E = 0$, and the stopping time is equal to infinity; 3) $R_0\dot{R}_0 + 8\nu < 0$, i.e., $Re > 8$; then the denominator of the integrand of Eq. (2.6) is negative during the entire time of the convergence of the cavity, collapse occurs, and $E = 2\pi\rho_1\nu^2(Re - 8)^2R_0$ and $\dot{R} \sim R^{-3/2} \to -\infty$ as $R \to 0$, just as in an ideal incompressible fluid.

The problem of the collapse of a spherical bubble in a viscous liquid has been discussed in a somewhat different formulation in [8]. Here the pressure p_0 under whose influence collapse of the cavity occurs is specified at infinity, i.e., in a formulation similar to Rayleigh's problem of the collapse of a spherical cavity in an ideal incompressible fluid. It is also found in [8] that the nature of the motion depends on the value of the Reynolds number, which is now defined as $Re = \frac{R_0}{\nu}\sqrt{\frac{p_0}{\rho_1}}$. When $Re > Re^*$, where Re^* is some critical number, collapse occurs, and the velocity of the cavity boundary $\dot{R} \to -\infty$ as $R \to 0$ according to the same law as in Rayleigh's problem. When $Re < Re^*$, the collapse of the bubble occurs slowly in an infinite time. In the intermediate case when $Re = Re^*$, the bubble collapses in a finite time, and the velocity $\dot{R}$ grows without limit as $R \to 0$, but more weakly than R^{-1}. Numerical integration of the equations in [8] gives a value of $Re^* = 8.4$ for the critical Reynolds number.

And so in contrast to motion with central symmetry, collapse to zero radius never occurs in the case of the inertial motion of a cylindrical shell of viscous fluid. It is also evident from Eq. (1.9) that if the pressure of the detonation products which acts on the outer surface of the shell drops to zero in a finite time, then collapse of the shell does not occur – it is stopped, and the inner surface of the shell never reaches the axis. Thus, the viscosity of the material of actual shells can be the principal cause, completely eliminating accumulation in devices with cylindrical symmetry. This fact must be taken into account in a number of physical devices which use the effect of the collapse of cylindrical shells (for example, magnetic course generators and so on).

Experimental verification of the stopping of the cylindrical shell at a certain distance from the symmetry axis in the case of explosive squeezing was carried out with x-ray pulse equipment. Copper tubes surrounded on the outside by a layer of explosives (TH 50/50 alloy) were used in the experiments. The detonation wave slips along the outer surface of the shell. Due to the large difference in the velocities of the detonation wave (7.5 km/sec) and the radial collapse (0.5-1.5 km/sec) one can consider the collapse process of the tube to be one-dimensional with cylindrical symmetry to high accuracy. The use of a sliding detonation wave permits recording in a single frame various temporal stages of the collapse of the cylindrical shell.

If one converts to a coordinate system attached to the front of the detonation wave, then it is clear that the cross sections of the tube farther from it will be in later stages of collapse, since $t=x/D$, where x is the distance from the detonation wave front to the tube cross section in question and D is the velocity of the detonation wave. The use of this procedure permitted clear recording in the experiments of the stopping of the inner surface of the shell at a certain distance from the axis of symmetry.

The collapse process of a copper tube ($R_0=9$ mm, $R_{10}=10$ mm) under the action of a layer of explosives is presented in Fig. 3a, b; the detonation wave front is moving from above to below. The x-ray photographs of the collapse process of the tube in Fig. 3a differ from the x-ray photographs of Fig. 3b in that in the first case an earlier stage of the collapse is presented and with a smaller initial velocity ($\dot{R}_0 \simeq 1$ km/sec) than in the second case ($\dot{R}_0 \simeq 1.6$ km/sec). The times are measured from the instant the explosives are fired by a detonator and are 8.7 and 14.3 μsec, respectively, for the first and second frames of Fig. 3a and 13.4, 16.3, 23.2, and 33.5 μsec for the sequence of frames of Fig. 3b. It is evident in the second frame of Fig. 3a and the first frame of Fig. 3b that the tube, having attained a minimum inner radius not equal to zero at some cross section, then expands. Dispersal of the shell starts in the next frames of Fig. 3b after the stage with minimum radius, and in the later frames the dispersal is accompanied by fracture, loss of continuity, and the appearance of instabilities which distort the axisymmetric shape of the dispersing shell.

Striving to obtain a stopping radius R_* large enough for high measurement accuracy imposes a restriction on the Reynolds number $Re=R_0|\dot{R}_0|/\nu$. For example, for shells for which $R_{10} \simeq 1.1\, R_0$, it follows from Eq. (2.3) that one should have $Re \leq 20$ if it is necessary to have a stopping radius of the inner surface of the order of $0.1\, R_0$. One can determine the viscosity of metals and other condensed materials from Eq. (2.3) and measurements on photographs (see Fig. 3a, b) of the initial velocity $\dot{R}_0$ and the inner stopping radius R_* :

$$\nu = \frac{R_0 |\dot{R}_0|}{4} \left[\sqrt{\frac{\ln\left(\dfrac{R_{10}^2 - R_0^2}{R_*^2} + 1\right)}{2\ln\dfrac{R_{10}}{R_0}}} - 1 \right]^{-1}.$$

For copper at deformation rates of $\sim 10^5$ sec^{-1} the value of the kinematic viscosity coefficient is found to be equal to $(1.5-1.8)\cdot 10^4$ cm^2/sec, which exceeds the value of the kinematic viscosity from the solution of the problem of explosive squeezing of a cylindrical shell. The reason for this discrepancy evidently consists of the fact that all the kinetic energy changes into heat by the instant of stopping. The shell layers adjacent to the inner surface are heated especially strongly. Vaporization and dispersion of the inner layers by the axis can begin just before their stopping, and the stopping radius recorded on the x-ray photograph will have an exaggerated value. The inner channel frequently turns out to be smeared.

§3. Heating up of a viscous cylindrical shell occurs upon its collapse to the axis as a result of the dissipation of kinetic energy.

Dependences obtained from (2.2) are presented in Fig. 4 of the dimensionless quantities – velocity of the inner radius $\dot{R}/\dot{R}_0$ and the kinetic energy E/E_0 – as a function of the dimensionless inner radius R/R_0 for a copper shell for which $R_0=9$ mm, $R_{10}=11.7$ mm, and $\nu=0.7\cdot 10^4$ cm^2/sec. Curves 3 correspond to an initial velocity $\dot{R}_0=1$ km/sec, curves 2 to $\dot{R}_0=2$ km/sec, and curves 1 to $\dot{R}_0=3$ km/sec. It follows from consideration of these curves that the fraction of the kinetic energy converted into heat is small right up to values $R/R_0=$ 0.5-0.7, and the collapse velocity is almost unchanged and equal to the initial value. Significant liberation of heat is observed prior to the stage of shell stopping, and all the kinetic energy changes into heat at the instant of stopping.

Let us estimate the temperature and its distribution with respect to shell thickness as a function of the time. We will again consider inertial motion. We obtain from Eq. (2.2) the equation of motion for the inner radius R of the shell:

$$\dot{R}=\frac{R_0\dot{R}_0\sqrt{\ln\frac{R_{10}}{R_0}}+4\nu\left(\sqrt{\ln\frac{R_1}{R}}-\sqrt{\ln\frac{R_{10}}{R_0}}\right)}{R\sqrt{\ln\frac{R_1}{R}}}. \tag{3.1}$$

The strength of the dissipation forces per unit volume is, according to (1.8),

$$N=\frac{d\varepsilon'}{dt}=4\mu\frac{R^2\dot{R}^2}{r^4}, \tag{3.2}$$

where r is the independent variable ($R \leq r \leq R_1$) and ε' is the dissipation energy per unit volume. We will follow a particle located in the interior of the cylindrical shell and having an initial radius r_0($R_0 \leq r_0 \leq R_{10}$). It follows from the mass conservation law (1.4') that $r^2(t)=R^2(t)+r_0^2-R_0^2$, and Eq. (3.2) for a moving particle with initial coordinate r_0 takes the form

$$\frac{d\varepsilon}{dt}=4\nu\frac{R^2\dot{R}^2}{(R^2+r_0^2-R_0^2)^2}, \tag{3.3}$$

where ε is the specific dissipation energy converted into heat, and $\varepsilon=0$ in Eq. (3.3) at $t=0$. Integrating (3.1) and (3.3) together, we find the temperature increment in the adiabatic approximation for the particle r_0 to be

$$\Delta T=\frac{4\nu}{c}\int_0^t\frac{R^2\dot{R}^2dt}{(R^2+r_0^2-R_0^2)^2},$$

where c is the specific heat of the shell material.

For numerical calculation the shell was divided into 10 equal intervals with respect to thickness at the initial time. Thus, the calculation was performed for 11 points, two of which belong to the inner and outer surfaces of the shell. The calculations of the temperature distribution in the shell (without taking phase transitions into account) were performed for copper, with $\nu=0.7\cdot10^4$ cm²/sec and $c=3.82\cdot10^6$ ergs/(g·deg).

The results of the calculation of the temperature distribution in a copper shell with respect to its thickness is shown at various times in Fig. 5. The initial shell parameters are as follows: $R_0=10$ mm, $R_{10}=11$ mm, and $\dot{R}_0=1$ km/sec.

The temperature distribution with respect to thickness of a copper shell ($R_0=9$ mm, $R_{10}=11.7$ mm) is given in Fig. 6 at the instant at which the inner surface of the shell attains a radius of 1 mm; the curves refer to different initial shell velocities and to different times. The temperature values obtained are rather high, and the temperature of the inner surface and the shell layers adjacent to it will be still higher by the stopping time in the viscous fluid model used here. If one compares Figs. 4 and 6 (both are for a shell with $R_0=9$ mm and $R_{10}=11.7$ mm), then by the time the inner radius of the shell attains a radius of 1 mm the "rapid" shell has more than 60% of its kinetic energy left, and the other two have 50% and about 20%.

The calculation of the temperature of the inner surface of the "slow" shell $\dot{R}_0=1$ km/sec, which is carried out to a radius $R=0.0715$ mm, which is almost equal to the stopping radius $R_*=0.0708$ mm, shows that the temperature rises to $13.4\cdot10^4$ °K at the time $t=8.16\,\mu$sec, and the velocity of the inner surface is equal to 40 m/sec at this time. A temperature of several tens of thousands of degrees, for example, is attained in condensed media only upon the passage of very strong shock waves. In the case of shock compression of lead by a factor of 2.2 the material behind the front is heated up to a temperature of 26,400°K [5], the pressure behind the shock front is higher than $4\cdot10^3$ kbar, and the thermal pressure amounts to 32% of the total.

Let us imagine the order of magnitude of the thermal pressure if heating of a copper shell takes place with constant volume, which is valid, since a heating up by $\Delta T=3.4\cdot10^4$ °K occurs during a time appreciably less than $2\,\mu$sec (see Fig. 6). We will use the relationship which relates the value of the thermal pressure to the thermal energy:

$$p_T=\Gamma(v)\varepsilon_T/v=\Gamma(v)c_VT/v\approx\Gamma(v_1)c_VT/v_1,$$

where Γ is the Gruneisen coefficient, c_V is the specific heat at constant volume, and $v_1=1/\rho_1$ is the specific volume under normal conditions. For copper at $T=3.4\cdot10^4$ °K the value of the pressure turns out to be higher than $3 \cdot 10^3$ kbar. Such high pressures create a shock wave in the shell material which propagates toward the outer layers and forces the shell to expand. Of course, the model under discussion cannot take account of all the complexities of the convergence process of actual metal shells toward the axis, but a number of physical effects described above are qualitatively explained.

The process of one-dimensional convergence of shells with cylindrical symmetry has been realized experimentally in the device shown in Fig. 7a. The cylindrical shell 6 being investigated ($R_{10}=10.5$ mm) surrounded by a layer 5 of TH 50/50 explosive material 5 mm thick was enclosed in a conical Duralumin generator 4, which excited a cylindrical detonation wave simultaneously over the entire surface of the explosives 5 along a length of 60 mm. The firing of the explosive layer 3, which accelerates the generator, is carried out by the detonator 1. Separation of the explosives away from the detonator towards the explosives layer 3 is carried out by means of an explosive layer surrounding the inert insert 2 made of a plastic cone and a steel disk in the base of the cone. The process of the collapse and dispersion of a copper tube ($R_0=10$ mm) is shown in Fig. 7. The initial velocity is of the order of 1.7-2 km/sec. The times are measured from the instant of firing and are 13, 19, 21, and 27 μsec for the sequence of frames shown.

A photograph is shown in Fig. 8 of the dispersion of a thicker iron tube ($R_0=9.5$ mm) 27 μsec after the device shown in Fig. 7a was fired. The thinner copper tube disperses into layers perpendicular to the symmetry axis by this time. The dome-shaped feature in Fig. 8 appeared due to an additional metal ring inserted into the lower part of the tube for a complete guarantee of the free outflow of air from the inner cavity during the process of shell collapse. A loss of stability of the initial shape of the cylindrical shell is noted in the expansion stage in both photographs (see Figs. 7 and 8). One can assume that this stability loss of the shell shape is caused by a rapid heating of the metal at constant volume already in the collapse stage, as a result of which axial forces appear which exceed the critical Eulerian force. Then the shell shape is determined by dynamic stability loss, which was first analyzed in [9] for elastic rods and shells.

Due to the unloading from the end surface of the explosives 5, which accelerates the shell being investigated, the collapse process of the tube at some section is far from uniform with cylindrical symmetry. The lower part of the tube of Fig. 7c and the upper parts of the tube of Fig. 3a, b collapse at some variable angle towards the symmetry axis. At the same time conditions for the collision of shell elements may be realized, which results in the formation of cumulative jets. We note that the ideal incompressible fluid model always predicts the formation of compact cumulative jets, whereas it is known that jets are formed under definite collision conditions. It is necessary to discuss the compressibility of the shell material in order to clarify the criterion for jet formation. The effect of compressibility on the formation of a jet is discussed in [10]. The flow pattern is the symmetrical collision of two jets at an angle 2β for a glancing collision of two plates in the coordinate system attached to the line of collision of the plates. It is known from gasdynamics that for a stream impinging on a wall at an angle β there exists a maximum angle β_{max}, which when exceeded results in the absence of an associated shock wave.

Thus, a flow without a cumulative jet is possible only when an associated shock wave is located at the point of collision. A cumulative jet is always formed in the case of an outgoing shock wave. This means that if the velocity of the incoming stream is subsonic, then a jet is always formed, and if it is supersonic, then a jet is formed when $\beta > \beta_{max}$ and is absent when $\beta < \beta_{max}$. This criterion is refined and supplemented in [11]. It is shown that it is applicable not only to colliding plates but also to conical shells. In addition, it has been established experimentally and by numerical calculations that the jets formed are monolithic in the case of a subsonic velocity of the incoming stream, but they are not compact for a supersonic velocity when $\beta > \beta_{max}$, and they break up into individual small particles.

One can generalize the criterion of jet formation if one changes to the laboratory coordinate system. In the general case if the phase velocity of the collision point of the shell elements on the symmetry axis is less than the local speed of sound in the vicinity of the collision point (and perturbations can depart in front of the shell), then a collision occurs with the formation of a jet. In the opposite case jet formation does not occur. This criterion is valid both for the plane and axisymmetric cases of collision.

One can see that in the case of one-dimensional collapse of cylindrical shells (it is realized in the device of Fig. 7) the velocity of the collision point of shell elements along the symmetry axis is equal to infinity and there should be no cumulative jets formed at all from this part of the cylindrical shell. Nevertheless, results are given in [12] on the production of cumulative jets of ultrahigh velocity (up to 90 km/sec) from cylindrical shells. The maximum velocities attained depend on the shell material and the diameters of the shell and charge. In addition, the formation of two jets was observed: a high-velocity one and the main one. The density of the high-velocity jet turns out to be of the order of $10^{-4}-10^{-3}$ g/cm^3 [12, 13]. The gaseous nature of the material of the high-velocity jet suggests that vaporization of material occurs as a result of the strong heating of the shell in the collapse process. The vaporized material of the inner shell layers flows out freely along the symmetry axis right up until complete collapse and forms the high-velocity jet. The main jet is evidently produced by virtue of an edge effect (see Fig. 7c) in the case of a supersonic velocity of the incoming stream when $\beta > \beta_{max}$. It is a stream of the smallest metal particles [12, 13], which is in good agreement with the refined criterion of jet formation [11]. A third jet is formed from the lowest tube elements (see Fig. 7d) with a density equal to the density of the material, and this jet is capable of damaging an obstacle. It is formed in the case of a subsonic velocity of the incoming stream [10]. The velocity measured for the leading elements of this jet turns out to be equal to 9.7 km/sec (see Fig. 7d).

An attempt is made in [13, 14] to discuss the high-velocity and main cumulative jets as the outflow of a highly compressed metal into a vacuum.

LITERATURE CITED

1. S. A. Kinelovskii, N. I. Matyushkin, and Yu. A. Trishin, "The convergence of an incompressible ring to the center under the action of the products of an explosion," in: The Dynamics of a Continuous Medium [in Russian], No. 5, Izd. Inst. Gidrodinam. Sibirsk. Otd. Akad. Nauk SSSR, Novosibirsk (1970).
2. S. A. Kinelovskii, N. I. Matyushkin, and Yu. A. Trishin, "The motion of a cylindrical piston toward the center," in: The Dynamics of a Continuous Medium [in Russian], No. 5, Izd. Inst. Gidrodinam. Sibirsk. Otd. Akad. Nauk SSSR, Novosibirsk (1971).
3. S. A. Kinelovskii, N. I. Matyushkin, and Yu. A. Trishin, "The motion of a cylindrical piston surrounded by a layer of expanding gas," in: The Dynamics of a Continuous Medium [in Russian], No. 7, Izd. Inst. Gidrodinam. Sibirsk. Otd. Akad. Nauk SSSR, Novosibirsk (1971).
4. F. A. Baum, K. P. Stanyukovich, and B. I. Shekhter, The Physics of Explosion [in Russian], Fizmatgiz, Moscow (1959).
5. Ya. B. Zel'dovich and Yu. P. Raizer, The Physics of Shock Waves and High Temperature Hydrodynamic Phenomena, Academic Press (1970).
6. A. A. Deribas, The Physics of Hardening and Welding by Explosion [in Russian], Nauka, Novosibirsk (1972).
7. A. A. Il'yushin and P. M. Ogibalov, Elastoplastic Deformations of Hollow Cylinders [in Russian], Izd. Mosk. Univ., Moscow (1960).
8. E. I. Zababakhin, "Phenomena of unlimited accumulation," in: Fifty Years of Mechanics in the USSR [in Russian], Vol. 2, Nauka, Moscow (1970).
9. M. A. Lavrent'ev and A. Yu. Ishlinskii, "Dynamical modes of the stability loss of elastic systems," Dokl. Akad. Nauk SSSR, 65, No. 6 (1949).
10. J. Walsh, R. Shreffler, and F. Willig, "Limiting conditions for jet formation in high-velocity collisions," J. Appl. Phys., 24, No. 3 (1953).
11. P. Chou, J. Carleone, and R. Karpp, "Criteria for jet formation from impinging shells and plates," J. Appl. Phys., 47, No. 7 (1976).
12. W. Koski, F. Lucy, R. Shreffler, and F. Willig, "Fast jets from collapsing cylinders," J. Appl. Phys., 23, No. 12 (1952).
13. N. P. Novikov, "High-velocity cumulative jets," Zh. Prikl. Mekh. Tekh. Fiz., No. 6 (1962).
14. N. P. Novikov, "Some properties of high-velocity cumulative jets," Zh. Prikl. Mekh. Tekh. Fiz., No. 1 (1963).